Environmental Science and Pollution Research (2020) 27:7538–7548
https://doi.org/10.1007/s11356-019-07404-z

RESEARCH ARTICLE

Mechanism of phosphorus mobility in sediments with larval (*Propsilocerus akamusi*) bioturbation

Wenming Yan[1] · Musong Chen[2] · Ling Liu[1] · Tingfeng Wu[2] · Yi Zhang[1] · Han Wang[1,2] · Xigang Xing[3] · Kongming Fan[4]

Received: 5 March 2019 / Accepted: 13 December 2019 / Published online: 29 December 2019

Abstract

The effects of chironomid larval (*Propsilocerus akamusi*) bioturbation on sediment phosphorus (P) mobility were studied over the course of 34 days using the indoor larval cultivation method on in situ sediment cores. High-resolution dialysis (HR-Peeper) and diffusive gradients in thin films (DGT) techniques were used to record fine-scale changes of soluble and DGT-labile P and iron (Fe) concentrations in the sediment. The larval-driven irrigation of the overlying water into their burrows significantly increased the oxygen penetration depth (OPD) and redox state (*E*h) in sediments. In addition, the soluble and DGT-labile P and Fe decreased with the increase of OPD and *E*h in larval-bioturbated sediments. The greatest decrease in the mean concentration of SRP, soluble Fe, and DGT-labile P in the *Propsilocerus* group was observed on Day 15 of the experiment, with a decrease by over half of the mean concentration of the control group. Furthermore, two-dimensional measurements of DGT-labile P concentration showed notable reductions of DGT-labile P around larval burrows. The DGT-induced fluxes in sediments (DIFS) model also exhibited a much longer response time (420 s) and a much higher rate of P adsorption (0.002 s^{-1}) in the bioturbation sediments than those in the control sediments (116 s and 0.009 s^{-1}, respectively). A significant correlation was shown for DGT-labile P and DGT-labile Fe. We conclude that Fe(II) oxidation and its enhanced adsorption were the major mechanisms responsible for the decrease of soluble and DGT-labile P in sediments.

Keywords Lake · Sediments · Bioturbation · Phosphorus · Iron

Introduction

Phosphorus (P) is the key nutrient causing lake eutrophication. An increased accumulation of P in lakes from farm runoff, industrial effluents, and sewage dramatically impairs lake ecosystems and can cause widespread eutrophication of lake water (Elser and Bennett 2011; Stone 2011). Some studies have reported that controlling P has succeeded in reducing eutrophication in many lakes (Carpenter 2008; Schindler et al. 2008). However, reducing P inputs has also been shown to be unsuccessful in controlling the eutrophication in some lakes (Michalak et al. 2013; Paerl et al. 2014). High internal loading of P from lake sediments is the major reason for most of these unsuccessful cases (Conley et al. 2009). High internal loading of P maintains the eutrophication of the lake, causing ecosystem recovery to be delayed by 10–15 years (Chen et al. 2018). Phosphorus mobility in sediments can be affected by the change of environmental factors in sediments including pH, dissolved oxygen (DO), redox state (*E*h), temperature, hydrodynamic disturbance, and faunal bioturbation (Chen et al. 2015; Jiang et al. 2008).

Faunal bioturbation includes all transport processes by macrobenthos in sediments including burrow building and particle reworking (Kristensen et al. 2012). Chironomid larvae (e.g., *Propsilocerus akamusi*) build U-shaped burrows in sediments and introduce oxygen-rich overlying water into these holes. The Fe(II) in sediment around the burrow is oxidized to Fe(III) oxyhydroxides and adsorbs P with the increase of

Responsible editor: Vedula VSS Sarma

✉ Musong Chen
mschen@niglas.ac.cn

[1] State Key Laboratory of Hydrology-Water Resources and Hydraulic Engineering, Hohai University, Nanjing 210098, China

[2] State Key Laboratory of Lake Science and Environment, Nanjing Institute of Geography and Limnology, Chinese Academy of Sciences, Nanjing 210008, China

[3] General Institute of Water Resources and Hydropower Planning and Design, Ministry of Water Resources, Beijing 100120, China

[4] The Huaihe River Commission of the Ministry of Water Resources P.R.C, Anhui Province, Bengbu 233000, China

oxygen in sediments (Chen et al. 2015; Lewandowski et al. 2007). This hypothesis has been supported by the decrease of dissolved Fe(II) and soluble reactive phosphorus (SRP) in pore water in the larval bioturbation sediments and lowers the release flux of P from sediment to the overlying water (Lewandowski and Hupfer 2005; Lewandowski et al. 2002, 2005; Reitzel et al. 2013; Schaller 2014; Zhang et al. 2010). In addition, some studies have shown that larval bioturbation can accelerate the mineralization and degradation of organic matter, further promoting the release of P (Andersson et al. 1988; Gallepp 1979). However, Meysman et al. (2006) found that the effect of larvae on P release was not significant. Thus, debate remains regarding the effect that larval bioturbation has on the release of P in sediments, which hinders our understanding of the role of lake sediment in geochemical processes. Furthermore, small-sized larvae are roughly 1 mm in size, and their burrow entrances have a diameter of 2 mm. Therefore, a high-resolution sampling method is required to reflect the changes of P surrounding the larval burrow.

In recent years, high-resolution (mm level) in situ passive sampling techniques, such as the diffusive gradients in thin films (DGT) technique and high-resolution dialysis (HR-Peeper), have solved this problem. This is particularly true with respect to the high resolution of the DGT technique using zirconium oxide (Zr-oxide) binding gel to measure the P reaching the micrometer level (Ding et al. 2013, 2015). These techniques allow for a more microcosmic, in situ, and multidimensional description of interface characteristics. Based on Fick's first law, the DGT technique uses the concentration gradient formed between the diffusion layer and the liquid phase. The concentration of available elements measured by DGT is interpreted as its mean concentration at the surface of the DGT device over the deployment time, which is calculated from the accumulated mass (Davlson and Zhang 1994). The HR-Peeper technique was based on traditional peeper techniques and on pore water dialysis. The HR-Peeper technique uses a dialysis membrane to separate the deionized water from the pore water. After diffusion equilibrium, the water samples in each chamber are collected and analyzed to determine the SRP and soluble Fe(II) (Teasdale et al. 1995). Recently, Lewandowski and Hupfer (2005) and Xu et al. (2012) improved the existing peeper technique, increasing the resolution from cm to mm scale and shortening the equilibration time to 48 h.

This study used DGT and HR-Peeper techniques to examine the effect of larval bioturbation on P mobility in sediments. High-resolution concentration profiles (one- and two-dimensional profiles of P and one-dimensional profiles of Fe) were obtained from our sediments, and their relationships were analyzed to reveal the bioturbation mechanisms of P mobility within sediments.

Materials and methods

Sampling area

Lake Dazong, China (119°43′11″–119°50′34″E, 33°7′54″–33°13′36″N), was selected as our research area (Fig. 1). Lake Dazong has an average depth of 1.02 m and is 5.5 km wide and 6 km long. The lakeshore is mainly composed of mud and sand, while bottom material consists of soft muddy clay in the west and solid silt clay in the east. The majority of the lake has been designated as an aquacultural area, which primarily cultivates fish, shrimp, and crab. As a result of these practices, the water body of Lake Dazong has experienced intense eutrophication. During our field investigation, a total of 12 species of zoobenthos were collected from the sampling site location in the center of the lake (Fig. 1), including 2 oligochaetes (134 ind. m^{-2}), 7 larval *P. akamusi* (470 ind. m^{-2}), and 3 molluscs (201 ind. m^{-2}). The total density of the zoobenthos was found to be 805 ind. m^{-2} in the sampling site, with larval *P. akamusi* (470 ind. m^{-2}) accounting for 58% of the zoobenthos. Thus, larval *P. akamusi* dominated in the sampling site and were consequently selected as research subjects for this study, which investigated the effects of bioturbation on P mobility in sediments.

Experiment design

In total, 12 sediment cores were collected from one sampling site location in the center of Lake Dazong (Fig. 1), using a gravity corer (length × internal diameter = 50 cm × 9 cm) in sediments at depths of at least 30 cm. The oxygen, *E*h, soluble Fe(II), and SRP values in the sampling site were 6 mg L^{-1}, 300 mV, 0.06 mg L^{-1}, and 0.03 mg L^{-1} in the overlying water, respectively, whereas they were 1.5 mg L^{-1}, 250 mV, 0.2 mg L^{-1}, and 0.07 mg L^{-1} in the pore water at the upper 10 mm of the sediments, respectively. The overlying water at the sampling site was collected using a 50-ml polyethylene barrel. A Petersen grab was used to sample the laboratory cultivation of *P. akamusi* larvae at the sampling site. Samples were delivered to the laboratory within 3 h. Subsequently, sediment cores were divided into 2-cm intervals. The same layer sediments were put together and filtered (0.6 mm diameter) to remove the zoobenthos. About 12 layers (24 cm high) were filled into 12 cores (length × internal diameter = 30 × 9 cm) according to their original depth. Sediment made up the bottom 24 cm of the cores, while the remaining 6 cm were filled with the overlying water. Twelve sediment cores were divided evenly into two tanks (45 cm high) and submerge-cultured using a siphon on the collected overlying water. Cultivation conditions were simulated in the two tanks by creating a 12:12 light/dark cycle at 15 °C. In addition, the tanks were pumped with air at a rate of 5 min/h to maintain oxygen saturation in the water column during incubation.

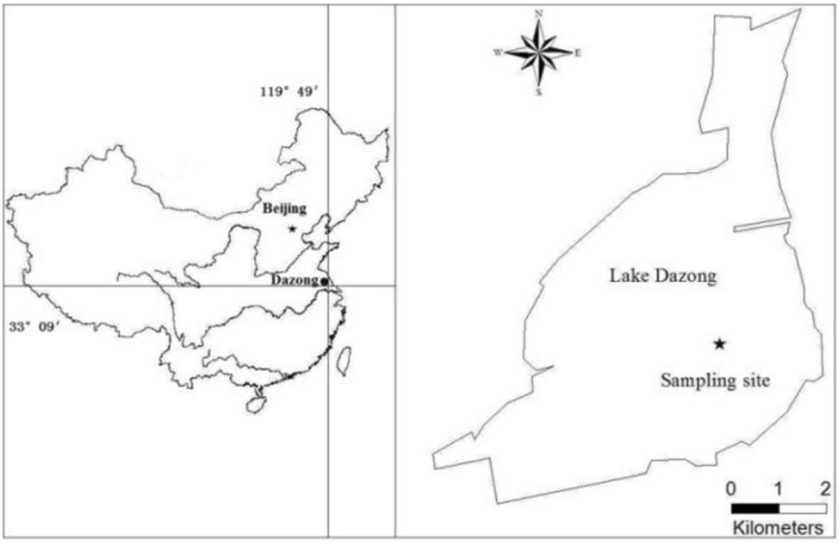

Fig. 1 Sampling site in Lake Dazong

After 14 days of cultivation, larval *P. akamusi* (12 larvae per core, approaching the population density of 470 ind. m^{-2} found at the sampling site) were introduced to six sediment cores in one tank and labeled as the *Propsilocerus* group. No zoobenthos were added into the other tank, which was set as the control group. The oxygen penetration depth (OPD) in sediments was 2.4 mm after 14 days of cultivation (Fig. 2). This value was similar to the mean OPD of 12 months from February 2016 to January 2017 at 2.28 mm in the sediments of Lake Taihu reported by Ding et al. (2018). Therefore, after 14 days of cultivation, the oxygen level in sediments was similar to that in situ.

Sampling and analysis

Samples were collected on Days 5, 15, 26, and 34 following *Propsilocerus* introduction. There was no survival of larval *P. akamusi* after 34 days. For each time point, microelectrodes were used to measure the dissolved oxygen (DO), *E*h, and pH in the *Propsilocerus* and control group sediments. Next, the HR-Peeper device was installed, and, after 24 h, the DGT (equipped with Zr-oxides and ZrO-Chelex binding gel, respectively) was added. The system was kept at equilibrium for another 24 h, followed by the simultaneous removal of the HR-Peeper and DGT devices. Three cores were selected from each group, and the five P forms were measured, including total P (TP; concentrated HCl-extractable P), inorganic P (IP), organic P (OP), non-apatite inorganic P (NAIP; indicating P bound to Fe, Mn, and Al oxides and hydroxides), and apatite P (AP; indicating P bound to Ca). These were measured in every other 2-cm layer, using the Standards Measurements and Testing Program of the European Commission (SMT) method (Ruban et al. 2001). The HR-Peeper measured the SRP and soluble Fe(II) in pore water, and DGT measured the labile P and labile Fe in the sediment. SRP and labile P were measured using molybdenum blue colorimetry (Murphy and Riley 1962), while soluble Fe(II) and labile Fe were measured using the phenanthroline colorimetric method (Tamura et al. 1974).

Data analyses

The concentrations of labile P and labile Fe measured by DGT (C_{DGT}) were calculated using the following formula (1):

$$C_{DGT} = M\Delta g/DAt \quad (1)$$

where Δg is the thickness of the diffusive layer, D is the diffusion coefficient of P (D_p) and Fe (II) (D_{Fe}) in the diffusion layer, A is the contact area (1.8 mm^2) of the DGT measurement window and sediments, t is the deployment time (24 h), and M is the P and Fe (II) accumulation in the binding gel during 24 h (Davison and Zhang 2012; Ding et al. 2013; Xu et al. 2013).

The DGT-induced fluxes in sediments (DIFS) model were used to calculate the kinetics of P remobilization from sediment solids (Harper et al. 2000). After obtaining the input index R (ratio of labile P to SRP) and K_d (distribution coefficient) values, T_C (exchange process response time) was calculated using the DIFS model to represent the time needed for the perturbed system to reach 63% equilibrium. The rate constants k_1 (the rate constant of P adsorption) and k_{-1} (the rate constant of P desorption) were then calculated using Formulas 2–3.

$$k_{-1} = 1/T_c(1 + K_d P_c) \quad (2)$$

$$k_1 = k_{-1}/K_d P_c \quad (3)$$

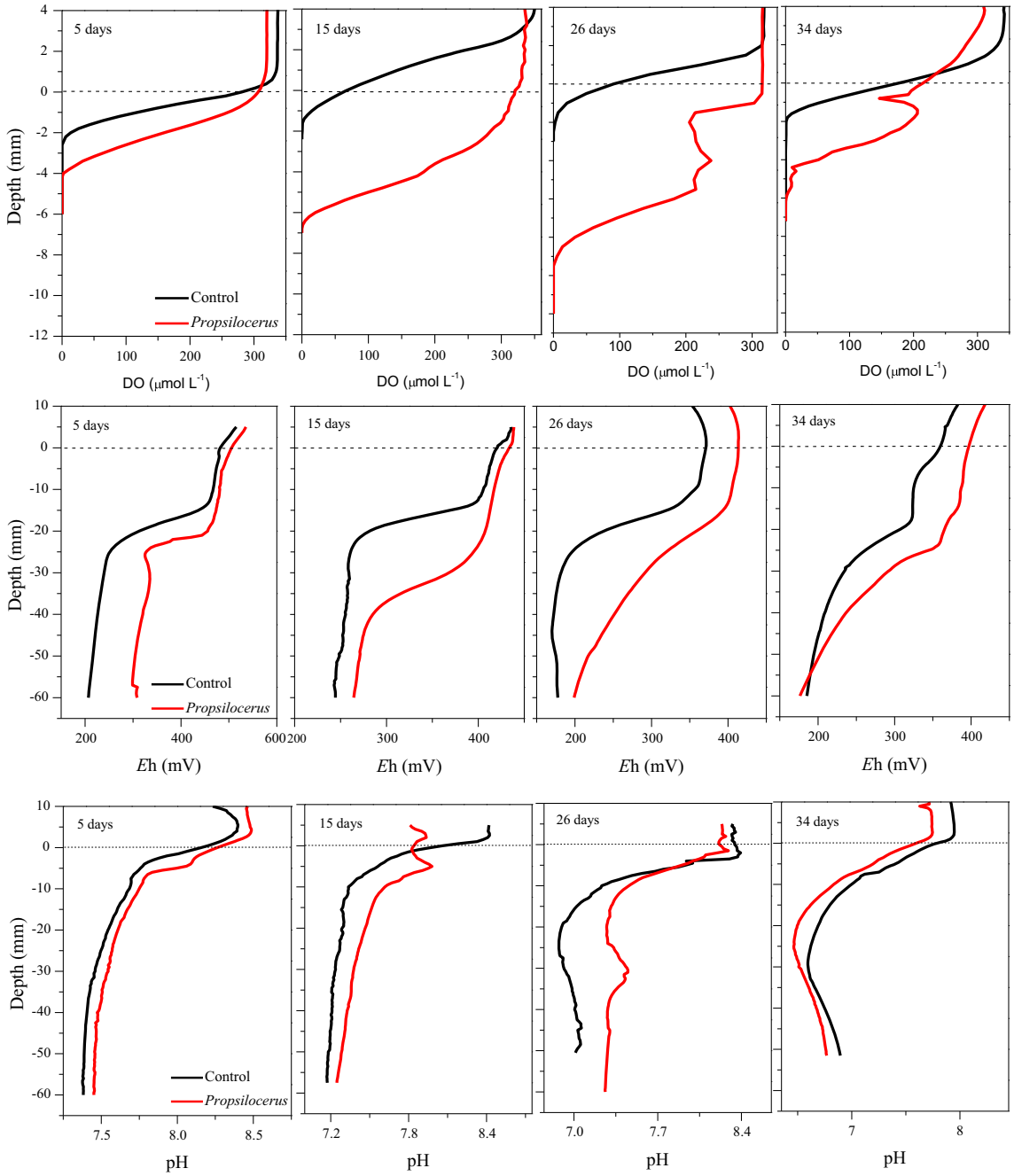

Fig. 2 DO, Eh, and pH profiles in sediments of control and *Propsilocerus* group for Days 5, 15, 26, and 34 (The data of DO, *E*h, and pH on Days 5 and 15 are from Yang et al. 2016 and Yan et al. 2017)

The DO, pH, *E*h, P flux, pore water soluble P and Fe, sediment labile P and Fe, and P fractionation between different treatments were compared using one-way repeated ANOVA. Where a significant difference existed between the two groups ($p < 0.05$), Tukey's post hoc test was used to analyze the level of the significant difference between the two groups at each time point. All significant differences are marked in the respective figures as *($p < 0.05$), **($p < 0.01$), and ***($p < 0.001$). All statistical analyses were performed using SPSS17.0 (SPSS, USA).

Results

The changes of DO, pH, and *E*h in sediments

As shown in Fig. 2, larval *P. akamusi* in our tanks built U-shaped burrows in the bottom sediments, introduced oxygen-rich overlying water to the burrows, and changed the redox conditions nearby. Furthermore, larval bioturbation significantly increased the OPD in sediment ($p < 0.05$). On Days 5, 15, 26, and 34, OPD in the *Propsilocerus* group (4.0, 6.6, 9.0,

and 6.0 mm, respectively) was significantly deeper than in the control group (2.4, 2.0, 2.0, and 3.2 mm, respectively). From Day 5 onward, OPD in the *Propsilocerus* group deepened successively. Furthermore, the greatest bioturbation occurred on Day 26 (Tukey's HSD test, $p < 0.001$) and then gradually decreased (Fig. 2). These results were in accordance with previous reports (Peter and Dirk 2006; Zhang et al. 2010). Thus, larvae increased the OPD by building U- or J-shaped burrows in the sediments and adding oxygen-rich overlying water for respiration (Chen et al. 2015).

Larval bioturbation significantly increased the redox potential (*E*h) ($p < 0.05$). On Days 5, 15, 26, and 34, the average *E*h in the *Propsilocerus* group (388, 356, 320, and 312 mV, respectively) was higher than that in the control group (318, 309, 252, and 273 mV, respectively) by a respective 22%, 15%, 27%, and 14%. Furthermore, the largest increment occurred on Day 26 (Tukey's HSD test, $p < 0.001$; indicating the strongest larval bioturbation during this period) and then gradually decreased (Fig. 2). Thus, *Propsilocerus* introduced a continuous supply of oxygen-rich overlying water into the burrows, which caused an *E*h increase in the pore water. The resultant variation of *E*h was consistent with that of the DO.

Larval bioturbation slightly increased the pH of sediments ($p < 0.05$) (Fig. 2). On Days 15 and 26, the sediment pH values (7.46 and 7.44, respectively) in the *Propsilocerus* group were higher than those in the control group (7.23 and 7.13, respectively). Furthermore, on Days 5 and 34, the sediment pH in the *Propsilocerus* group showed no significant difference (when comparing the pH values at each depth) ($p > 0.05$) from that of the control group.

Phosphorus mobility in sediments with larval bioturbation

As shown in Fig. 3, P fluxes in the four sampling time points of the control group were positive, indicating the release of P from the cultivated sediment into the overlying water. In contrast, P fluxes in the first three sampling time points of the *Propsilocerus* group were negative, indicating the adsorption of dissolved P by sediments. On Day 34, the P fluxes of the two groups showed a significant difference ($p < 0.01$), indicating that larval bioturbation also had an effect on the P flux in the overlying water at this time point.

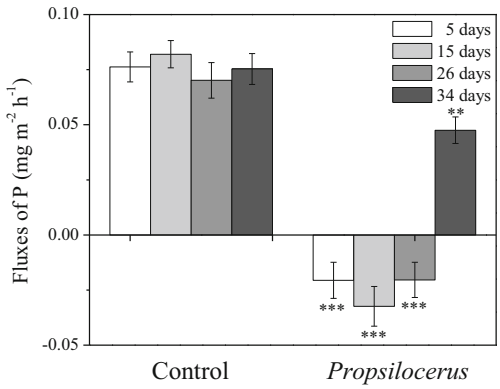

Fig. 3 Fluxes of P across the sediment–water interface. ** and *** indicate the significant difference between the control and *Propsilocerus* groups at $p < 0.01$ and $p < 0.001$, respectively

In the first three sampling time points, larval bioturbation significantly decreased the pore water SRP and labile P concentrations ($p < 0.05$) (Fig. 4). The biggest SRP decrease (57%) occurred on Day 15 (Tukey's HSD test, $p < 0.001$), while the effective depth occurred from the sediment-overlying interface to 100 mm below the surface. Following Day 15, the effects of larval bioturbation gradually decreased, and on Day 34, the SRP between the two groups was virtually the same ($p > 0.05$). The largest labile P decrease (68%) occurred on Day 15 (Tukey's HSD test, $p < 0.001$), while the effective depth was from the sediment-overlying interface to 80 mm below the surface. Following Day 26, the effects of larval bioturbation gradually decreased to a reduction ratio of 57% on Day 34. Thus, larval bioturbation increased the pore water OPD and *E*h (Fig. 2), changed the sediment redox conditions, and directly affected the pore water SRP and labile P concentrations. Furthermore, the variations of SRP and labile P were consistent with those of DO and *E*h. These results were in accordance with those of Lewandowski et al. (2007) and Zhang et al. (2010).

The two-dimensional spatial distribution of labile P concentrations showed that labile P concentrations in the control group were low from the sediment–water interface to a depth of −10 mm, increased steadily from −10 to −30 mm (maximum 0.25 mg L^{-1}), then remained stable until a depth of −80 mm, and decreased gradually from −80 to −100 mm (minimum 0.10 mg L^{-1}) (Fig. 5a). Labile P concentrations in the *Propsilocerus* group were generally lower than those of the control group. This indicates that larval bioturbation significantly affected the two-dimensional distribution of sediment labile P, with a larger reduction from the sediment–water interface to −70 mm. The two-dimensional labile P distribution in the *Propsilocerus* group showed an obvious U-shaped region on the left side—from the sediment–water interface to −70 mm (Fig. 5a). Labile P within this region was generally lower than both the surrounding area and in the center of this U-shaped region. The similarity between the shape of this region and the U-shaped *Propsilocerus* burrows indicates that this U-shaped region might have been larval bioturbation tracks. These results show that the high-resolution two-dimensional DGT technique, with Zr-oxide as the binding gel, accurately described the affected labile P during bioturbation.

The relative standard deviation (RSD) of the labile P concentration in the horizontal direction was calculated to reflect

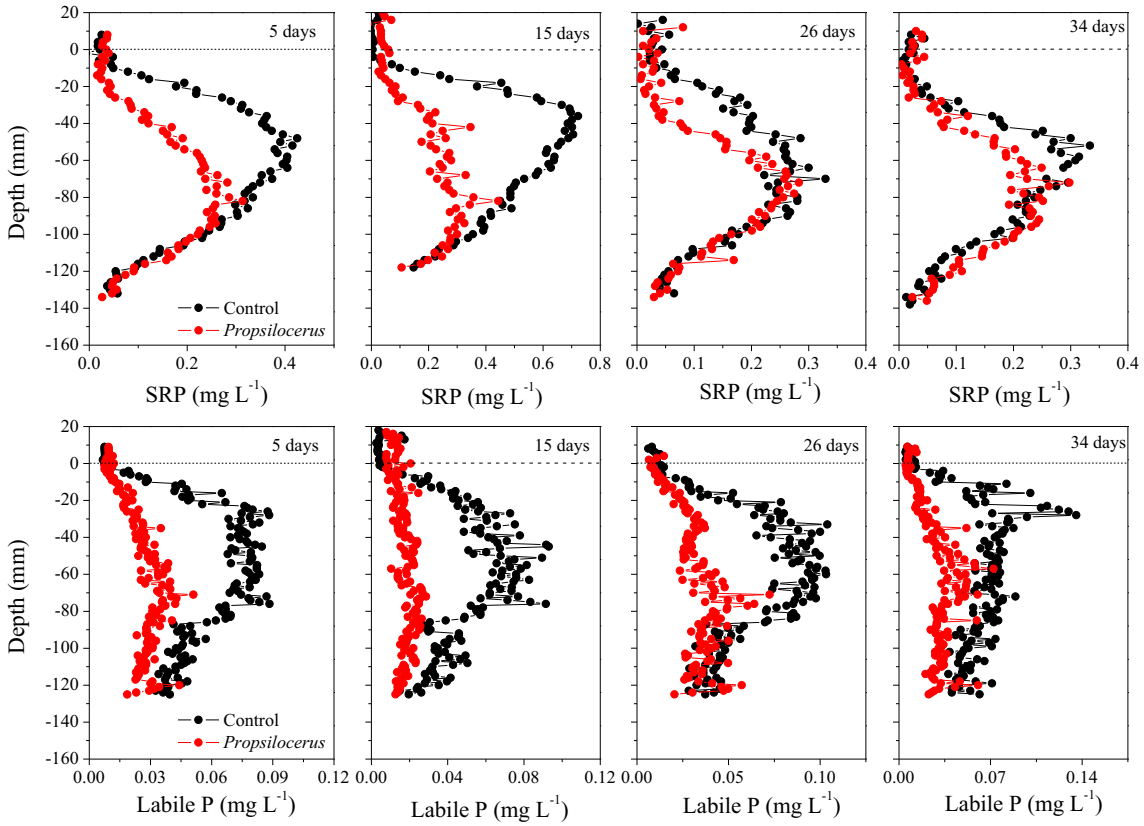

Fig. 4 Effects of larval bioturbation on SRP and labile P concentrations in sediment profiles (The data of SRP on Day 15 are from Yang et al. 2016)

the heterogeneity index of the horizontal labile P concentration distribution (Fig. 5b). Larval bioturbation significantly increased the heterogeneity index of labile P, with the three most significant bioturbation depths from 0 to −40 mm, from −49 to −76 mm, and from 79 to −111 mm. From 0 to −40 mm, the average horizontal heterogeneity index of sediment within the *Propsilocerus* group (0.38) was higher than those in the control group (0.16) by 138%, the highest impact detected. Furthermore, from −49 to −76 mm and from −79 to −111 mm, the average horizontal heterogeneity indexes of sediment in the *Propsilocerus* group (0.28 and 0.22, respectively) were higher than those in the control group (0.13 and 0.17, respectively) by a 115% and 29%, respectively.

After Days 15, 26, and 34 of *Propsilocerus* incubation, sediments were collected from a depth of 6 cm to the deposition column surface (in two columns from each group) and used for P classification experiments (Fig. 6). As shown in the figure, NAIP of the *Propsilocerus* group increased significantly ($p < 0.05$), while TP, IP, OP, and AP showed no significant changes ($p > 0.05$). The sediment NAIP represents the P bound to Fe, Mn, and Al oxides and hydroxides. The increase in NAIP concentration indicated that more P was bound to Fe, Mn, and Al oxides and hydroxides in the *Propsilocerus* bioturbation sediments. These results were consistent with those from the literature (Chen et al. 2015; Granéli 1979; Matisoff et al. 1985).

Iron mobility in sediments with larval bioturbation

The effects of larval bioturbation on soluble Fe(II) in sediment pore water were similar to those observed for SRP. In the first three sampling time points, larval bioturbation significantly decreased the soluble Fe(II) concentrations ($p < 0.05$) (Fig. 7). The greatest reduction (49%) occurred on Day 15 (Tukey's HSD test, $p < 0.001$), with the affected depth ranging from the sediment–water surface to −60 mm. Following Day 15, the effects of larval bioturbation decreased gradually, and on Day 34, the soluble Fe(II) between the two groups was virtually equivalent ($p > 0.05$). Thus, larval bioturbation showed no long-term effects on soluble Fe(II). These results were consistent with those of Zhang et al. (2010). In addition, the variation of soluble Fe(II) was consistent with that of DO and *E*h (Fig. 2).

On Days 5, 15, and 26, larval bioturbation significantly decreased the labile Fe concentrations ($p < 0.05$) by 78%, 56%, and 71%, respectively. The largest reduction occurred on Day 5 (Tukey's HSD test, $p < 0.001$), with the affected depth ranging from the sediment–water surface to −60 mm, and on Days 15 and 26, the affected depth reached −90 mm. Furthermore, on Day 26, the effects of larval bioturbation diminished, and on Day 34, the reduction of the labile Fe concentration reached 39%. These findings were consistent with those of DO and *E*h (Fig. 2).

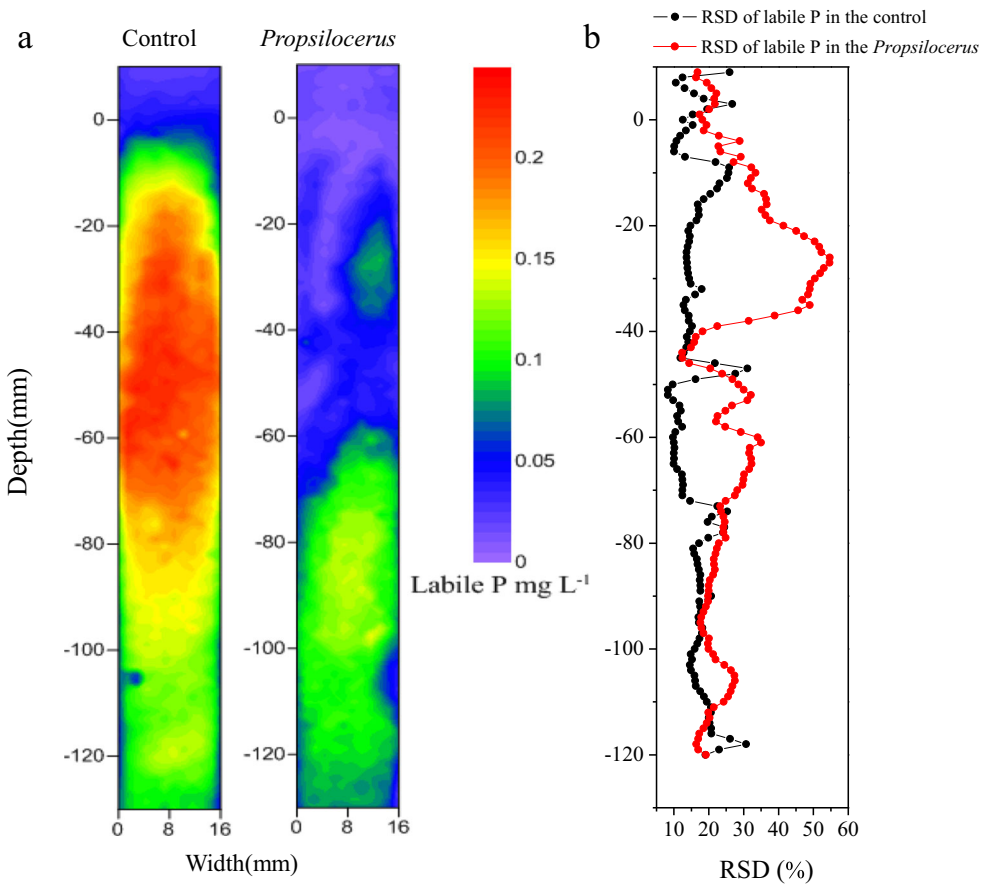

Fig. 5 Effects of larval bioturbation on labile P concentration in sediment on Day 26 after incubation of the *Propsilocerus*. (a) Two-dimensional labile P concentration profiles in sediment. (b) Changes in labile P concentration horizontal heterogeneity index (reflected by the relative standard deviation, RSD) with sediment depth

The relationship between P and Fe

Pearson correlation analysis showed that on Days 5, 15, 26, and 34, labile P and labile Fe were positively correlated ($p < 0.01$; Table 1). SRP and soluble Fe(II) were positively correlated in the first two and three sampling time points of the *Propsilocerus* group and control group, respectively.

Kinetics of P mobility in the sediments

The DIFS model was used to simulate the supplemental dynamic capabilities of surface (0–4 cm) sediment P (from the solid phase to the liquid phase) on Day 15 in the control and *Propsilocerus* groups. The inputs and outputs of the DIFS model are shown in Table 2. The R, k_1, and k_{-1} values in

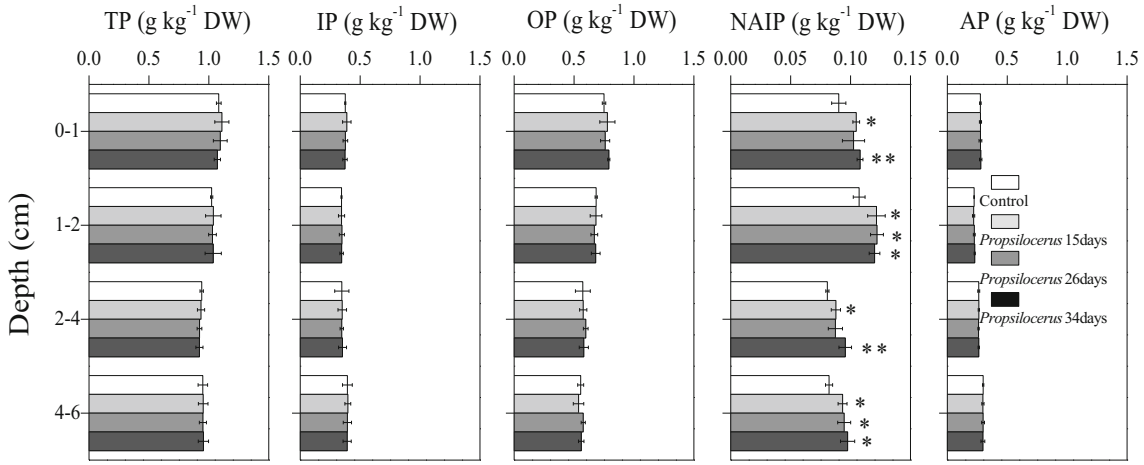

Fig. 6 Fractionation of P in the upper 6 cm of sediments, with and without larval bioturbation

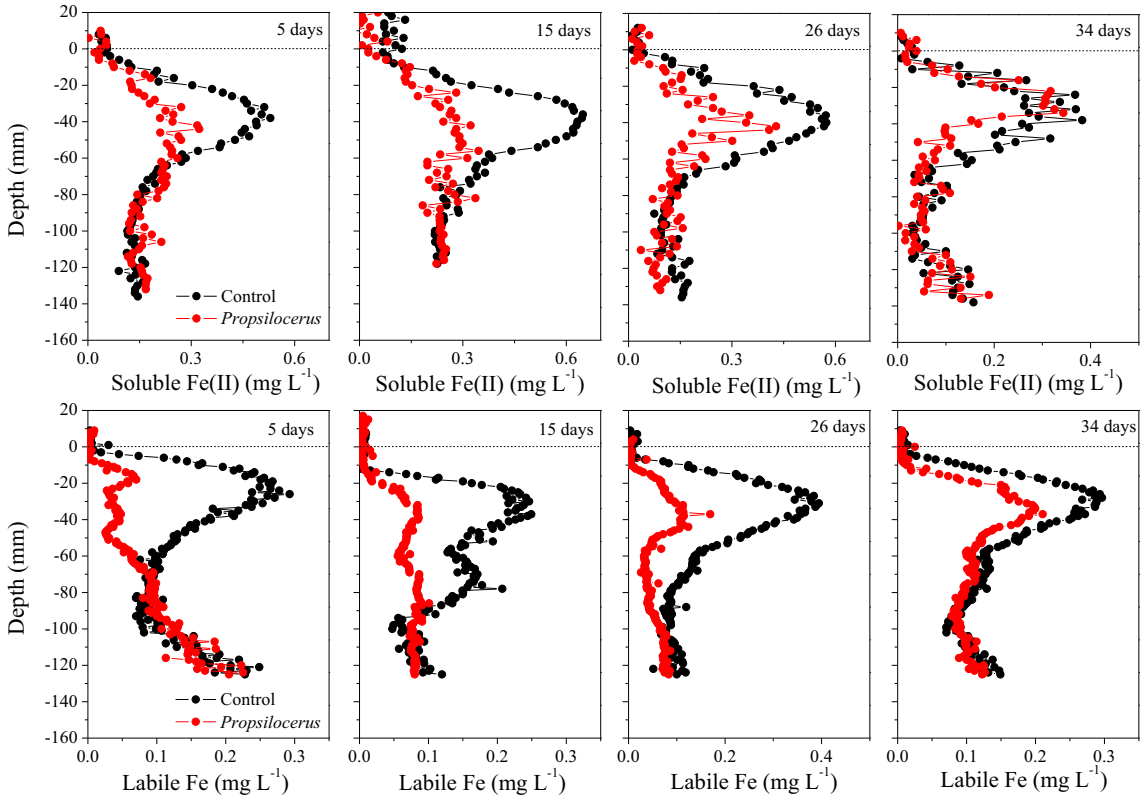

Fig. 7 Effects of larval bioturbation on soluble Fe(II) and labile Fe concentrations in sediment profiles (The data of soluble Fe(II) on Day 15 are from Yang et al. 2016)

the *Propsilocerus* group were lower than those in the control group. The R, k_1, and k_{-1} values in the control group were 1.2, 4.5, and 10 times those of the *Propsilocerus* group, respectively. In contrast, the values of K_d and T_c in the *Propsilocerus* group were 3.5 and 3.6 times higher than those in the control group, respectively.

Table 1 Correlation analyses between soluble/labile P and Fe

Groups		Days	r	p
SRP vs. soluble Fe(II)	*Propsilocerus*	5	0.529^{***}	< 0.001
		15	0.801^{***}	< 0.001
		26	0.076	0.527
		34	-0.411^{***}	< 0.001
	Control	5	0.649^{***}	< 0.001
		15	0.915^{***}	< 0.001
		26	0.399^{***}	< 0.001
		34	0.033	0.787
Labile P vs. labile Fe	*Propsilocerus*	5	0.511^{***}	< 0.001
		15	0.618^{***}	< 0.001
		26	0.239^{**}	< 0.01
		34	0.435^{***}	< 0.001
	Control	5	0.377^{***}	< 0.001
		15	0.705^{***}	< 0.001
		26	0.564^{***}	< 0.001
		34	0.763^{***}	< 0.001

Discussion

To facilitate respiration and the filtering of phytoplankton from the overlying water, *Propsilocerus* irrigated the oxygen-rich overlying water into their U-shaped burrows, which increased the oxygen penetration depth in the sediments (Lewandowski and Hupfer 2005; Lewandowski et al. 2007; Zhang et al. 2010) (Fig. 2). Oxygen irrigated into these burrows subsequently diffused, forming an oxidized layer around the burrow. Within this oxidized layer, the oxidation of Fe(II) into Fe(III) oxyhydroxides turned the surroundings

Table 2 DIFS model input and output parameters

DIFS	Parameters	Unit	*Propsilocerus*	Control
Input	R	–	0.248	0.287
	K_d	$cm^3\ g^{-1}$	3.59×10^3	1.04×10^3
Output	T_c	s	420	116
	k_1	s^{-1}	0.002	0.009
	k_{-1}	s^{-1}	2.57×10^{-6}	2.62×10^{-5}

brown (Einsele 1936; Mortimer 1941) and thus decreased the labile Fe and soluble Fe(II) concentrations in sediments around the burrows (Fig. 7). The newly formed Fe(III) oxyhydroxides, with support from the significant positive correlation between soluble and labile P and Fe (Table 1), then adsorbed pore water SRP and labile P near the burrows (Mortimer 1941; Chen et al. 2019; Ding et al. 2016; Søndergaard et al. 2003). The adsorption of Fe(III) decreased the sediment labile P and SRP concentrations around the burrows (Fig. 4, 5a), increased the horizontal heterogeneity of sediment labile P (Fig. 5b), and allowed the fixing of the adsorbed SRP and labile P in the sediment particles. Furthermore, this increased the sediment non-apatite inorganic phosphorus (NAIP; Fig. 6) while decreasing the ability of sediment solid particle P to supplement SRP. Finally, it inhibited the release of sediment labile P and SRP and decreased the overlying water P flux (Chen et al. 2015; Lewandowski and Hupfer 2005; Lewandowski et al. 2007; Zhang et al. 2010) (Fig. 3). In the sampling site, the release of SRP to the water column was 30.6 mg m^{-2} (SRP concentration × water depth). The mean fluxes of P on Days 5 and 15 were 0.079 and − 0.027 mg m^{-2} h^{-1} in the control and *Propsilocerus* treatments, respectively (Fig. 3). In the control treatment, the release of SRP to the water column was 30.34 mg m^{-2} after 16 days, which was similar to that in situ. In the *Propsilocerus* treatment, the release of SRP to the water column was −10.37 mg m^{-2} after 16 days of bioturbation. This indicates that the SRP was absorbed at 10.37 mg m^{-2} after 16 days of *Propsilocerus* bioturbation. Therefore, the *Propsilocerus* bioturbation could decrease SRP release from sediments to the water column by 34% after 16 days.

The DIFS model results further demonstrated that the *Propsilocerus* bioturbation inhibited the release of sediment labile P and SRP. The *R* value reflects the supplemental capability of sediment particle-adsorbed P to pore water (Harper et al. 2000). The *R* value in the *Propsilocerus* group was lower than that in the control group (Table 2), indicating that the P supplemental capability (of sediment particle-adsorbed P to pore water) was slower in the *Propsilocerus* group than that in the control group. The K_d values indicated the P maintenance capability of the sediment system under equilibrium conditions (Zhou et al. 2005). K_d in the *Propsilocerus* group was found to be higher than that in the control group, which indicated the stronger P maintenance capability of the sediment in the *Propsilocerus* group. T_c was used to describe the equilibration time of the sediment system (Harper et al. 1998), and this value was higher in the *Propsilocerus* group than that in the control group. This shows that *Propsilocerus* bioturbation caused an increase in the equilibration time of the sediment system. Furthermore, the k_1 and k_{-1} values in the control group were higher than those in the *Propsilocerus* group. Thus, *Propsilocerus* bioturbation increased the system equilibration time by slowing the P adsorption and desorption rates of sediment solid particles (Chen et al. 2016). Overall, these results indicate that *Propsilocerus* bioturbation inhibited the sediment particle P release into pore water.

Conclusions

Using indoor-cultivated in situ sediment cores, combined with high-resolution DGT and HR-Peeper techniques, the P mobility in the bioturbated sediments was explored in the microscale. Results showed that P changes were primarily controlled by Fe oxidation adsorption. Respiration by larval *P. akamusi* introduced oxygen-rich overlying water to the U-shaped burrows and increased the OPD and *E*h in the sediment. Furthermore, this oxidized Fe(II) around the burrows into Fe(III) oxyhydroxides, increased the SRP and labile P adsorption capability of sediments around the burrow, and inhibited the supplemental abilities of P from sediment solids. This decreased the labile P and SRP concentrations in the sediment.

Funding information This work was supported by the National Key R&D Program of China (2017YFC0405205); National Natural Science Foundation of China (41701568, 41301531, 51279060, and 41673123); Key Research Program of Frontier Sciences, Chinese Academy of Sciences (QYZDJSSWDQC008); the "One-Three-Five" Strategic Planning of Nanjing Institute of Geography and Limnology, Chinese Academy of Sciences (NIGLAS2017GH04); Hubei Provincial Natural Science Foundation of China (2017CFB312); and the Fundamental Research Funds for the Central Universities (2017B20514).

References

Andersson G, Granéli W, Stenson J (1988) The influence of animals on phosphorus cycling in lake ecosystems. Hydrobiologia 170(1):267–284

Carpenter SR (2008) Phosphorus control is critical to mitigating eutrophication. P Nate Acad SCI USA 105(32):11039–11040

Chen MS, Ding S, Chen X, Sun Q, Fan X, Lin J, Ren M, Yang L, Zhang C (2018) Mechanisms driving phosphorus release during algal blooms based on hourly changes in iron and phosphorus concentrations in sediments. Water Res 133:153–164

Chen MS, Ding S, Liu L, Xu D, Han C, Zhang C (2015) Iron-coupled inactivation of phosphorus in sediments by macrozoobenthos (chironomid larvae) bioturbation: evidences from high-resolution dynamic measurements. Environ Pollut 204:241–247

Chen MS, Ding SM, Wu YX, Fan XF, Jin ZF, Daniel CWT, Wang Y, Zhang C (2019) Phosphorus mobilization in lake sediments: experimental evidence of strong control by iron and negligible influences of manganese redox reactions. Environ Pollut 246:472–481

Chen MS, Ding SM, Liu L, Xu D, Gong MD, Tang H, Zhang C (2016) Kinetics of phosphorus release from sediments and its relationship with iron speciation influenced by the mussel (*Corbicula fluminea*) bioturbation. Sci Total Environ 542:833–840

Conley DJ, Paerl HW, Howarth RW, Boesch DF, Seitzinger SP, Havens KE, Lancelot C, Likens GE (2009) Controlling eutrophication: nitrogen and phosphorus. Science 323(5917):1014–1015

Davison W, Zhang H (2012) Progress in understanding the use of diffusive gradients in thin films (DGT)–back to basics. Environ Chem 9(1):1–13

Davlson W, Zhang H (1994) In situ speciation measurements of trace components in natural waters using thin-film gels. Nature 367(6463):546–548

Ding SM, Chen MS, Gong MD, Fan XF, Qin BQ, Xu H, Gao SS, Jin ZF, Tsang DCW, Zhang CS (2018) Internal phosphorus loading from sediments causes seasonal nitrogen limitation for harmful algal blooms. Sci Total Environ 625:872–884

Ding SM, Han C, Wang Y, Yao L, Wang Y, Xu D, Sun Q, Williams PN, Zhang C (2015) In situ, high-resolution imaging of labile phosphorus in sediments of a large eutrophic lake. Water Res 74:100–109

Ding SM, Wang Y, Xu D, Zhu C, Zhang C (2013) Gel-based coloration technique for the submillimeter-scale imaging of labile phosphorus in sediments and soils with diffusive gradients in thin films. Environ Sci Technol 47(14):7821–7829

Ding SM, Wang Y, Wang D, Li YY, Gong M, Zhang C (2016) In situ, high resolution evidence for iron-coupled mobilization of phosphorus in sediments. Sci Rep 6:1–11

Elser J, Bennett E (2011) A broken biogeochemical cycle. Nature 478: 29–31

Einsele W (1936) Über die Beziehungen des Eisenkreislaufs zum Phosphatkreislauf eutrophen, im eutrophen See. Arch Hydrobiol 29:664–686

Gallepp GW (1979) Chironomid influence on phosphorus release in sediment-water microcosms. Ecology 60(3):547–556

Granéli W (1979) The influence of Chironomus plumosus larvae on the exchange of dissolved substances between sediment and water. Hydrobiologia 66(2):149–159

Harper MP, Davison W, Tych W (2000) DIFS—a modelling and simulation tool for DGT induced trace metal remobilisation in sediments and soils. Environ Model Softw 15(1):55–66

Harper MP, Davison W, Zhang H, Tych W (1998) Kinetics of metal exchange between solids and solutions in sediments and soils interpreted from DGT measured fluxes. Geochim Cosmochim Ac 62:2757–2770

Jiang X, Jin X, Yao Y, Li L, Wu F (2008) Effects of biological activity, light, temperature and oxygen on phosphorus release processes at the sediment and water interface of Taihu Lake, China. Water Res 42(8):2251–2259

Kristensen E, Penha-Lopes G, Delefosse M, Valdemarsen T, Quintana CO, Banta G.T (2012) What is bioturbation? The need for a precise definition for fauna in aquatic sciences. Mar Ecol Prog Ser 446: 285–302

Lewandowski J, Hupfer M (2005) Effect of macrozoobenthos on two-dimensional small-scale heterogeneity of pore water phosphorus concentrations in lake sediments: a laboratory study. Limnol Oceanogr 50(4):1106–1118

Lewandowski J, Kristina Rüter A, Hupfer M (2002) Two-dimensional small-scale variability of pore water phosphate in freshwater lakes: results from a novel dialysis sampler. Environ Sci Technol 36(9): 2039–2047

Lewandowski J, Laskov C, Hupfer M (2007) The relationship between Chironomus plumosus burrows and the spatial distribution of pore-water phosphate, iron and ammonium in lake sediments. Freshw Biol 52(2):331–343

Lewandowski J, Schadach M, Hupfer M (2005) Impact of macrozoobenthos on two-dimensional small-scale heterogeneity of pore water phosphorus concentrations: in-situ study in Lake Arendsee (Germany). Hydrobiologia 549(1):43–55

Matisoff G, Fisher JB, Matis S (1985) Effects of benthic macroinvertebrates on the exchange of solutes between sediments and freshwater. Hydrobiologia 122(1):19–33

Meysman FJR, Galaktionov OS, Britta G, Middelburg JJ (2006) Bioirrigation in permeable sediments: advective pore water transport induced by burrow ventilation. Limnol Oceanogr 51(1):142–156

Michalak AM, Anderson EJ, Beletsky D, Boland S, Bosch NS, Bridgeman TB, Chaffin JD, Cho K, Confesor R, Daloğlu I, DePinto JV, Evans MA, Fahnenstiel GL, He L, Ho JC, Jenkins L, Johengen TH, Kuo KC, LaPorte E, Liu X, McWilliams MR, Moore MR, Posselt DJ, Richards RP, Scavia D, Steiner AL, Verhamme E, Wright DM, Zagorski MA (2013) Record-setting algal bloom in Lake Erie caused by agricultural and meteorological trends consistent with expected future conditions. P Nate Acad SCI USA 110(16): 6448–6452

Murphy J, Riley JP (1962) A modified single solution method for the determination of phosphate in natural waters. Anal Chim Acta 27: 31–36

Mortimer CH (1941) The exchange of dissolved substances between mud and water in lakes. J Ecol 29:280–329

Paerl HW, Gardner WS, McCarthy MJ, Peierls BL, Wilhelm SW (2014) Algal blooms: noteworthy nitrogen. Science 346(6206):175–175

Peter S, Dirk DB (2006) Probing the microenvironment of freshwater sediment macrofauna: implications of deposit-feeding and bioirrigation for nitrogen cycling. Limnol Oceanogr 51(6):2538–2548

Reitzel K, Lotter S, Dubke M, Egemose S, Jensen SH (2013) Effects of phoslock (R) treatment and chironomids on the exchange of;nutrients between sediment and water. Hydrobiologia 703(1): 189–202

Ruban V, López-Sánchez JF, Pardo P, Rauret G, Muntau H, Quevauviller Ph (2001) Harmonized protocol and certified reference material for the determination of extractable contents of phosphorus in freshwater sediments – A synthesis of recent works. Fresen. J. Anal. Chem. 370(2-3): 224–228

Schaller J (2014) Bioturbation/bioirrigation by Chironomus plumosus as main factor controlling elemental remobilization from aquatic sediments? Chemosphere 107(2):336–343

Schindler DW, Hecky RE, Findlay DL, Stainton MP, Parker BR, Paterson MJ, Beaty KG, Lyng M, Kasian SEM (2008) Eutrophication of lakes cannot be controlled by reducing nitrogen input: results of a 37-year whole-ecosystem experiment. P Nate Acad SCI USA 105(32):11254–11258

Stone R (2011) China aims to turn tide against toxic Lake pollution. Science 333(6047):1210–1211

Søndergaard M, Jensen JP, Jeppesen E (2003) Role of sediment and internal loading of phosphorus in shallow lakes. Hydrobiologia 506-509:135–145

Teasdale PR, Batley GE, Apte SC, Webster IT (1995) Pore-water sampling with sediment peepers. Trac-Trend Anal Chem 14:250–256

Tamura H, Goto K, Yotsuyanagi T, Nagayama M (1974) Spectrophotometric determination of iron(II) with 1,10-phenanthroline in the presence of large amounts of iron(III). Talanta 21(4):314–318

Xu D, Wu W, Ding S, Sun Q, Zhang C (2012) A high-resolution dialysis technique for rapid determination of dissolved reactive phosphate and ferrous iron in pore water of sediments. Sci Total Environ 422(4):245–252

Xu D, Chen Y, Ding S, Sun Q, Wang Y, Zhang C (2013) Diffusive gradients in thin films technique equipped with a

mixed binding gel for simultaneous measurements of dissolved reactive phosphorus and dissolved iron. Environ Sci Technol 47(18):10477–10484

Yan WM, Ma L, Han W, Yang JL, Yang YQ (2017) Effects of the Chironomus plumosus on the redox characteristics of Sediment-water micro interface. J. Hohai Univ. 45(6):489–494.

Yang TT, Liu L, Chen MS, Yang YQ, Yan WM, Lu ZJ (2016) Influence of Chironomid Larvae Bioturbation on Phosphorus Concentrations of Micro Scale in Sediments-Water Interface. Water Resour. Power 34(12):69–73.

Zhang L, Gu X, Fanl C, Shang J, Shen Q, Wang Z, Shen J (2010) Impact of different benthic animals on phosphorus dynamics across the sediment-water interface. J Environ Sci-China 22(11):1674–1682

Zhou A, Tang H, Wang D (2005) Phosphorus adsorption on natural sediments: modeling and effects of pH and sediment composition. Water Res 39:1245–1254